

# Crack initiation and path prediction of float glass with various constrain conditions under thermal loading

Q. S. Wang, Y. Wang, J. H. Sun and L. H. He

State Key Laboratory of Fire Science, University of Science and Technology of China, Hefei 230026, P.R.China, email:pinew@ustc.edu.cn

**ABSTRACT.** *Thermal caused glass crack and fracture are very common in building fires. To disclose the different constrain effect on the glass crack initiation and crack propagations, five constrain cases were simulated and compared on the first crack time, crack propagation path and so on using a finite element program. The crack location and the growth are predicted using Coulomb-Mohr criterion and SIFs based mixed-mode criterion, respectively. The thermal stress distribution, crack initiation, and crack growth path were obtained and compared. It was found that the four edges fully constrained glass sustained longest time to crack, and then is the two edges constrained case. The one edge constrained glass is easiest one to crack, which is a dangerous glass install method used in the building windows. The free constrained glass also shows a longer time to crack than the one edge constrained condition. The crack propagation speed are same and with a velocities of 2003 m/s. These new knowledge are helpful to the building windows glass design.*

## INTRODUCTION

Glass crack and full out when exposing fire has been taken attention several decades ago, however, it was proposed as a scientific topic to study is from the year of 1986 at the first fire safety science symposium by Emmons [1]. After that, some experimental works were carried out to studied the glazing behavior exposing fires. The heat release rates, enclosure and local gas temperatures, heat flux distributions, glass surface temperatures, shaded glass temperatures thermally induced stains, crack bifurcation patterns and loss of integrity of the glazing assembly were systematically investigated by Shields et al. [2-5]. They found that the temperature difference at first crack is 80 °C [2-5]. Skelly et al. [6] proposed that the temperature difference between the central and the edge is 90 °C. Keskirahkonen produced the theoretical value is 70 °C [7]. Chow et al. [8] investigated the fire smoke effect on glass crack by experiment, and analyzed the thermal stress in theory. Xie et al. [9] conducted a series of full-scale experiments in the ISO 9705 fire test room using pool fires with different pan sizes, which were located at the center of the combustion room. The results suggest that the whole piece of toughened glass cracks and falls out completely when any region of the pane breaks.

Theoretical and simulation works are limited developed to investigate the glass crack under thermal or fire exposing. The theoretical work either on the general fracture

mechanics or on the general heat transfer. Their conjunction and application on the fire induced glass crack and fall out is few reported, especially on the finite element method to simulate the glass crack initiation and propagation.

The objective of this work is to investigate the glass thermal stress build up, crack initiation and propagation using finite element method. The effect of various constrained condition of glass on the crack were investigated and compared under thermal loading.

## THERMAL STRESS AND CRACK FORMULAS

### *Thermal Stress Model*

The thermal stress is calculated using the following Eq. 1 by finite element method.

$$(\lambda + 2G)\nabla^2 e - \alpha\nabla^2 T = 0 \quad (1)$$

where  $\lambda$  is Lamé coefficient, and  $G$  is shear modulus of elasticity,  $e$  is volumetric strain,  $\alpha$  is the thermal expansion coefficient, and  $\nabla$  is Laplacian.  $\lambda$ ,  $G$  and  $e$  are expressed as:

$$\lambda = \frac{E\nu}{(1+\nu)(1-2\nu)}, \quad G = \frac{E}{2(1+\nu)}, \quad e = \varepsilon_x + \varepsilon_y + \varepsilon_z$$

where  $\nu$  is Poisson's ratio,  $\varepsilon_x$ ,  $\varepsilon_y$  and  $\varepsilon_z$  are the strain in x, y and z directions.

### *Crack Models*

Crack occurs when the maximum and minimum principal stresses combine for a condition which satisfies the following Eq. 2:

$$\frac{\sigma_1}{S_{ut}} - \frac{\sigma_3}{S_{uc}} \geq 1 \quad (2)$$

where  $S_{ut}$  and  $S_{uc}$  represent the ultimate tensile and compressive strengths, and both  $\sigma_3$  and  $S_{uc}$  are always negative, or in compression.

SIFs based mixed-mode criterion is used mode to predict crack growth in present work. It assumes cracks start to grow once the following Eq. 3 for the stress intensity factors is satisfied.

$$\left(\frac{K_I}{K_{IC}}\right)^\alpha + \left(\frac{K_{II}}{K_{IIC}}\right)^\beta + \left(\frac{K_{III}}{K_{IIIC}}\right)^\gamma = 1 \quad (3)$$

where,  $K_I$ ,  $K_{II}$  and  $K_{III}$  are the stress intensity factors for the three fracture modes, respectively, which are obtained from the simulation.  $K_{IC}$ ,  $K_{IIC}$  and  $K_{IIIC}$  denote the individual fracture toughness values of the three fracture modes. The constant parameters  $\alpha$ ,  $\beta$  and  $\gamma$  should be empirically determined, we taken it as Eq. 4 [10].

$$\left(\frac{K_I}{K_{IC}}\right)^2 + \left(\frac{K_{II}}{K_{IIC}}\right)^2 = 1 \quad (4)$$

## STATEMENT OF PROBLEM AND SIMULATION PROCEDURE

### *Simulation Model of the Problem*

In building, the window glass is embedded into window frames for fixing, and about 2cm is shaded by the frame. In case of fire, the shaded area are not expose to the fire radiation directly, therefore, the temperature is lower than the central part of the glass. The central part of the glass temperature rising is mainly dominated by the radiation from the fires. The shaded area temperature rise is caused by the heat conduction from the central parts of the glass itself and the heated frame. In general, the shaded area temperature rise is smaller than that of the central parts of the glass. At the back side of the glass, the temperature rise is controlled by the heat conduction rate from the front side and heat convection rate to the environment. This temperature is smaller than that of the front part of the glass too. The temperature differences between the shaded part and the uncovered part, between back side and the front side will build up the thermal stress between them because of its expansion.

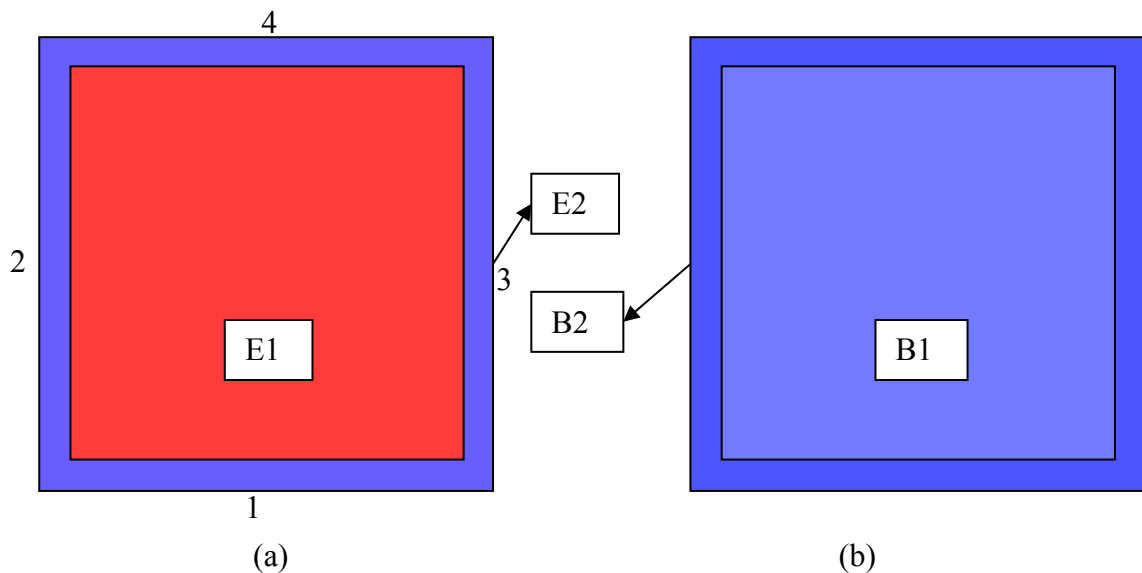


Fig. 1 Glass heated conditions. (a) E1 is exposing fire and E2 is shaded by frame; (b) B1 is the back side of fire and B2 is shaded by frame.

With the consideration of the heating condition of glass in case of fire, a kind of glazing situation was designed to investigate the thermal stress distribution and crack propagation as shown in Fig. 1. There are four parts for the glass to be considered in temperature rising, E1, E2, B1 and B2, respectively. E1 denote the glass exposing to the fire directly and E1 is shaded by frame at the same side. B1 means the glass back side and B2 is shaded by frame at the same side. At the central part (E1) of the glass, the temperature rising rapidly, and the other parts are rising slowly. The exact temperature rising plots are shown in Fig. 2, respectively.

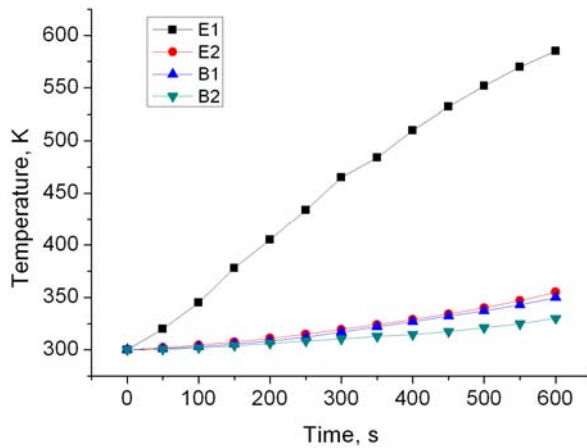


Fig. 2 Glass temperature rising history with time at four parts shown in Fig. 1.

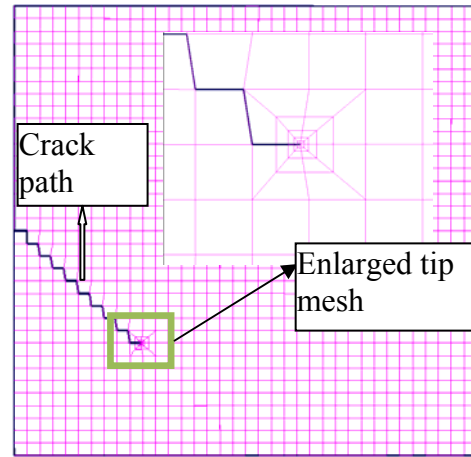


Fig. 3. Mesh subdivision for the simulation of crack growth.

Table 1. Glass properties [8] and other parameters used in simulation

Properties	Symbol	Value	Units
Thermal expansion co-efficient	$\alpha$	$8.0 \times 10^{-6}$	$K^{-1}$
Modulus of elasticity(Young Modulus)	E	$7.0 \times 10^{10}$	Pa
Poisson's ratio	$\nu$	0.25	--
Density	$\rho$	2520	$kg/m^3$
Ultimate tensile strength	$\sigma_{ut}$	$4.0 \times 10^7$	Pa
Ultimate compressive strength	$\sigma_{uc}$	$4.010^8$	Pa
Glass size	--	$0.006 \times 0.6 \times 0.6$	$m^3$
Shaded edge width	d	0.02	m
Mesh number	--	$2 \times 36 \times 36$	--
Time step	$\Delta t$	1	s

A glass is an inorganic non metallic material that does not have a crystalline structure. Typical glasses range from the soda-lime silicate glass for soda bottles to the extremely

high purity silica glass for optical fibers. Glass is widely used for windows, bottles, glasses for drinking, transfer piping and receptacles for highly corrosive liquids, optical glasses, windows for nuclear applications etc. etc. The practical tensile strength of glass is about 27MPa to 62 MPa. However, glass can withstand extremely high compressive stresses. Therefore, most glass breakage is due to tensile strength failure. Glass is weak in tensile strength is that it is normally covered in microscopic cracks which generate local stress concentrations. Glass does not possess mechanisms for reducing the resulting high localised stresses and so it is subject to rapid brittle fracture.

The soda-lime silicate glass is widely used in windows and it is a kind of brittle materials, which is selected in this work. This kind of glass properties and simulation parameters are shown in Table 1.

### ***Simulation Procedure***

The simulation in this study basically follows the method proposed by our previous study[11]. In this method, two models were employed, one is thermal stress model and another is crack model based on the stress model. In the thermal stress model, the finite element method was taken to simulate the dynamic thermal stress field using a Newmark time integration. And then to predict the crack occurrence by Coulomb-Mohr criterion. If the crack is initiated, the program will get into the crack model. In the crack model, five crack growth criteria are provided to predict the crack growth direction and crack length, where not only the stress intensity factors ( $K_I$ ,  $K_{II}$  and  $K_{III}$ ) but also the energy release rates ( $G_I$ ,  $G_{II}$  and  $G_{III}$ ) are calculated. Furthermore, the effects of stress re-distribution due to the crack extension are taken into account in order to properly estimate the stress intensity factors at an arbitrarily extended crack tip.

The calculation procedure is summarized as follows:

1. to generate analysis data including thermal loads and finite-element mesh for a given geometry,
2. to calculate the stress field with time step and predict the crack initiated or not, if yes, go to crack model, if not yet, loop into next time step,
3. after crack, to refine the crack tip mesh and calculate the stress intensity factors and energy release rates,
4. to predict the crack tip extension, crack direction and recreate the mesh,
5. to return step 3 before the geometry split into two parts.
6. to terminate the simulation when the body is split into two parts or finish the simulation time.

In the step-by-step finite-element calculations, an automatic mesh generation is required after crack. In order to avoid an excessive numerical cost, a proper mesh pattern is arranged in the vicinity of a crack tip by refining crack tip meshes. Only the elements surrounding the tip are refined by a fractal way. With the crack propagation, the refined tip mesh is moving too, and the ever refined elements back to the original mesh after the crack path through. Fig. 3 shows a typical example of the generated mesh.

## THERMAL STRESS AND CRACKING FORMATION OBTAINED BY SIMULATION

Five cases were simulated to investigate constrain effect on the glass thermal stress growth, crack initiation and propagation. The first case is that the glass edges are free, that is without constrain. The second case is that only one edge is constrained, the bottom edge 1 is constrained as shown in Fig. 1(a). The third case is that two side edges 2 and 3 are constrained. The fourth case is edges 1, 2 and 3 are constrained and the fifth case is that the four edges are constrained.

### *Without Constrain*

Without the constrain effect, the glass can expansion freely. At the central of glass as shown in Fig. 4(a), the first principal stress reaches to 65.7 MPa, the maximum second principal stress and third principal stress are 40.2 MPa and 4.1 MPa, respectively. By comparing with the ultimate tensile and compressive strength using Coulomb-Mohr criterion, the crack starts at the central of the glass. After that, the stress redistributed and the stress distribution is shown in Fig. 4(b). It can be seen that the stress concentration locates at the crack tips and large stress intensity factors are formed, which drives the crack growth further. The crack starts to propagate to two ways, one is going to the y direction and another one is going to negative z direction with small deviation to y direction as shown in Fig. 4(c). At last, one small “island” is formed caused the glass failure.

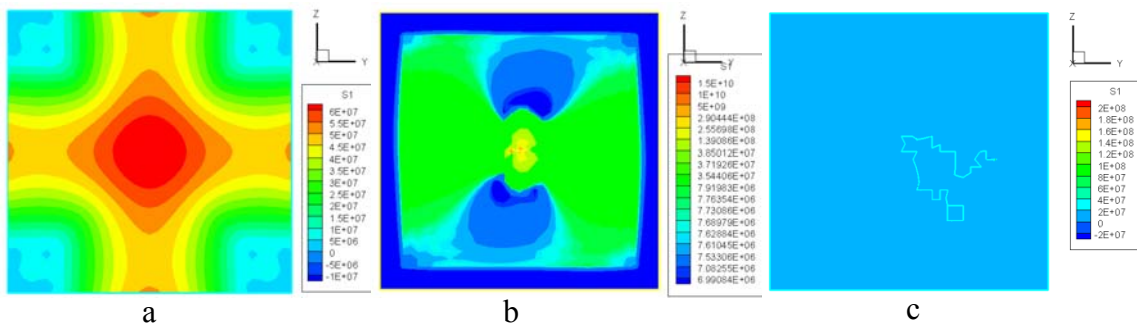


Fig. 4. Glass thermal stress distribution without constrain, (a) before crack, (b) after crack, and (c) the final crack path.

### *One Edge Constrained (Bottom Edge)*

When the bottom edge is constrained, as shown in Fig. 5, the first principal stress concentrates at the constrained edge, the maximum value reaches to 49.8 MPa before crack occurs. The second and third principal stresses are quite smaller than the first one. The crack starts at the bottom central of the constrained edges, and propagates to the negative y direction till to the edge of the glass.

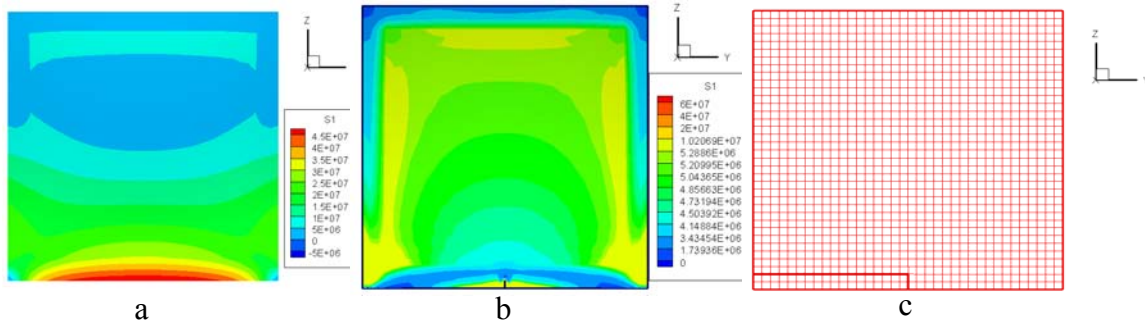


Fig. 5. Glass thermal stress distribution with one edge constrained, (a) before crack, (b) after crack, and (c) the final crack path.

### *Two Edges Constrained (Left and Right Edges)*

With two edges constrained, the first principal stress concentrates on the constrained edges. The stress increasing symmetrically at the two edges and reaches to the breaking stress as shown in Fig. 6. As this program only can simulate one crack growth, therefore only one of the location cracks when more locations concentrate the same stresses. As the glass is constrained at the edges, and then the central section is under compressive stress state, which arrest the crack propagating to the center. Therefore, the crack only can spread along the edges, and turn back to the edge after a short propagation as shown in Fig. 6(c).

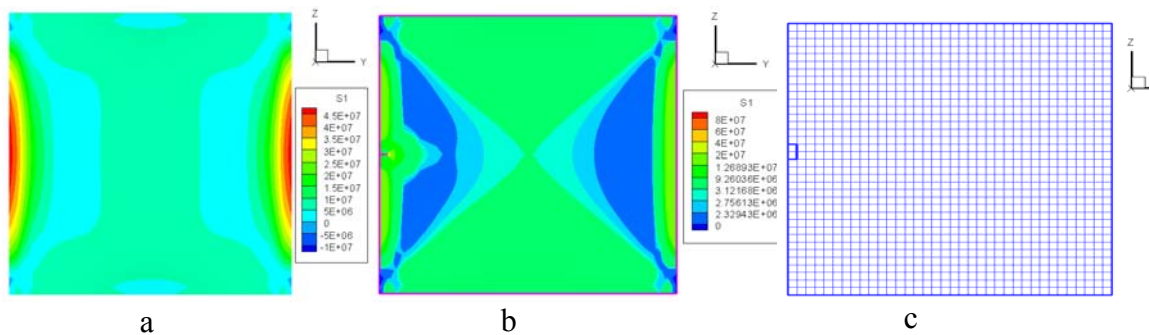


Fig. 6. Glass thermal stress distribution with two edges constrained, (a) before crack, (b) after crack, and (c) the final crack path.

### *Three Edges Constrained (Left, Right and Bottom Edges)*

With three edges constrained, the stress concentrates at the constrained three edges, it also increase symmetrically. Similar with two edges constrained condition, crack starts at one of the maximum tensile stress locations as shown in Fig. 7. And then, the strain energy is released around the crack tip as shown Fig. 7(b). However, the other two edges energy not released yet, therefore, there is a potential to release energy by creating new surface. The competitive result between the edge 1 (bottom) and edge 3

(right) is that the crack going to the corner between them, which is simulated as shown in Fig. 7(c).

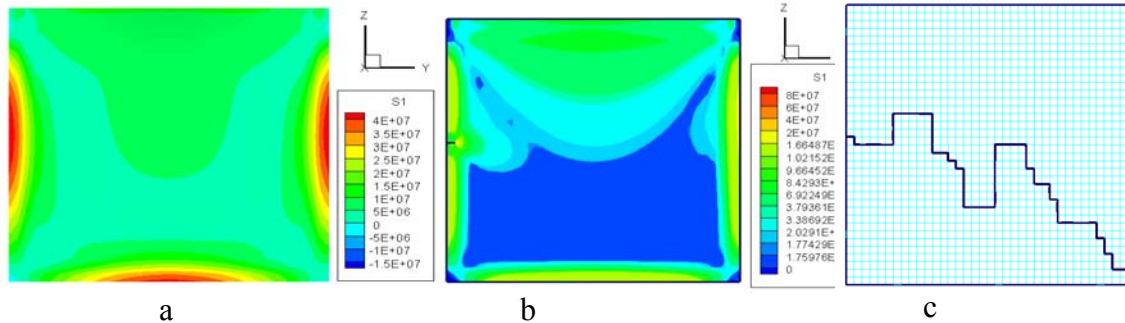


Fig. 7. Glass thermal stress distribution with three edges constrained, (a) before crack, (b) after crack, and (c) the final crack path.

#### ***Four Edges Constrained***

Under the four edges constrained, the stress growing synchronously around the four edges, and the maximum first principal stress appears at the center of four edges as shown in Fig. 8. After the crack is initiated, the strain energy around the tip is released, therefore, there is not tensile stress anymore, and then the crack is arrested without moving to the other edges as shown in Fig. 8(b). Finally, the crack turn back to the original edge, which is similar with two edges constrained case as shown in Fig. 8(c).

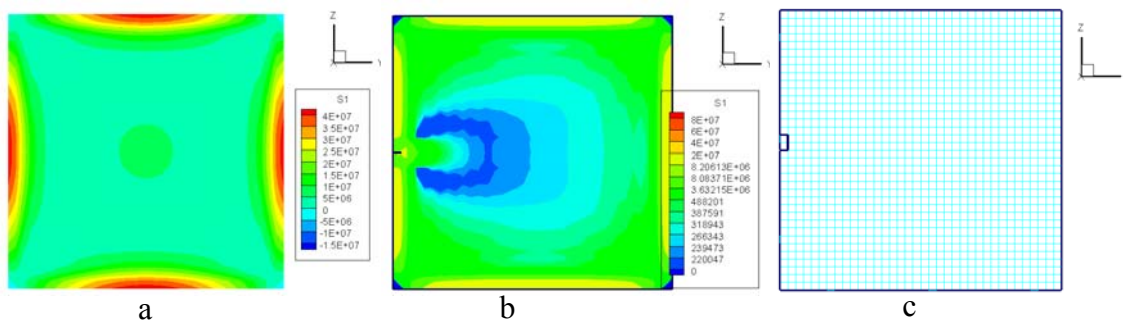


Fig. 8. Glass thermal stress distribution with four edges constrained, (a) before crack, (b) after crack, and (c) the final crack path.

### **COMPARISON AND DISCUSSIONS**

The above results show different crack behaviors under varying constrained conditions. Some key crack parameters were summarized and listed in table 2. The results of free constrained case is different with that of the constrained cases on the crack time, maximum first principal stress, temperature difference before crack. No obvious trend can be concluded, which is because that the edges can expansion freely without any



constrain, which is different with the constrained situations. For the constrained cases, the crack time is delayed with the constrained edges number increasing, and the temperature difference increasing as well. Under the constrained conditions, the constrained edges displacement are unchangeable, the glass expansion will force the glass to bend and drag the edges to the center. Therefore the constrained edges is dragged cause it under tensile condition. With more edges constrained, the glass can stand a longer time to crack, that is why the four edges constrained glass has longer crack time. The maximum first principal stress is decreasing with the constrained edges increasing. The crack length is various with each other except case 2 and case 4. Under the two and four edges constrained states, the energy are released near the crack tip, and it cannot extends to the other edges. For the three edges constrained glass, the crack starts at one of the constrained edges and the other two edges competitive result make the crack find a way in the middle of them. The crack velocity is same for these five cases with a value of 2003 m/s, which is close to the reported value of 2000 m/s [12].

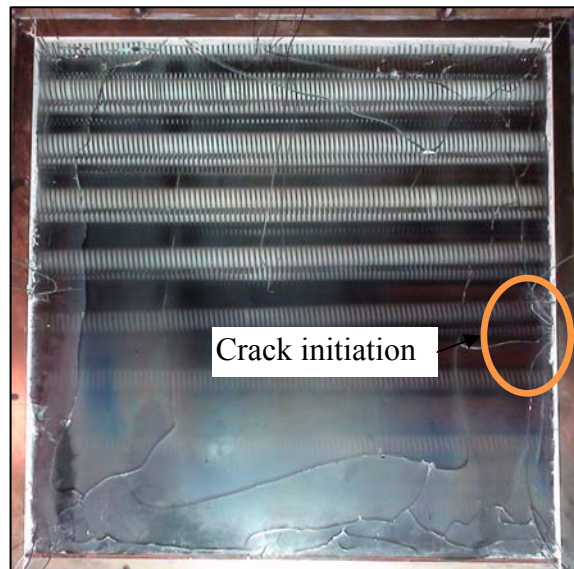


Figure 9. Final glass crack pattern under radiation heating of glass, glass size  $0.006 \times 0.6 \times 0.6 \text{ m}^3$ .

Table 2. Crack parameters under varying constrain conditions

Cases	1	2	3	4	5
Constrained edges	0	1	2	3	4
Crack time, s	59	51	70	72	74
Max $\sigma_1$ before crack, MPa	65.7	49.8	48.4	45.3	43.8
Temperature difference before crack, K	27.7	19.5	28.2	29.1	30.0
Crack length, m	0.50	0.3	0.067	0.967	0.067
Crack velocity, m/s	2003	2003	2003	2003	2003

To validate the simulation results generally, an experimental result is picked to compare with the simulation results. Fig. 9 shows one experimental result of glass crack under thermal heating. The glass size is  $0.006 \times 0.6 \times 0.6 \text{ m}^3$ . It can be seen the glass crack starts at the right center edge and propagate along the edge. The crack initiation location is same with the edges constrained cases. Most of the cracks are along with the edges to the edge or meet with other crack. Some bifurcation, multi-cracks propagation and junctions are observed further. The real case glass crack under thermal heating is very complicated and the current program is not enough to simulate the whole processes. However, the crack initiation location and single crack propagation path can be predicted.

## CONCLUSIONS

In the present paper, attention is focused on the thermal stress concentration, crack initiation and propagation of glass under heating with or without constrains. The thermal stress distribution is predicted by using a finite element program, where the step-by-step analyses are carried out. After the crack occurs, the crack tip mesh is refined and the automatic mesh is generate with the crack propagating. Without constrain, the crack occurs at the center of the glass under this designed thermal loads. Under the edges constrained condition, the crack occurs at the center of constrained edges. The crack turns back to the edge for the two and four edges constrained condition. The crack propagates along the edge for the one edge constrained case, and it propagates to the center of another constrained edges for the three constrained case. More works are required to simulate the multi-crack propagation to fit the real case glass crack propagation, bifurcation and junctions.

## ACKNOWLEDGEMENTS

This work is supported by the National Natural Science Foundation of China (Grant. No. 51120165001), National Basic Research Program of China(973 Program, Grant. No. 2012CB719700), and the Fundamental Research Funds for the Central Universities (Grant no. WK2320000004 and WK2320000014).

## REFERENCES

1. Emmons, H.W. The Needed Fire Science. In: Fire Safety Science-Proceedings of the First International Symposium. pp 33-53. 1986.
2. Shields, T.J., Silcock, G.W.H., and Hassani, S.K.S. (1997-98) *J APPL FIRE SCI* **7**,145-163.
3. Shields, T.J., Silcock, G.W.H., and Flood, M.F. (2001) *Fire Mater* **25**,123-152.
4. Shields, T.J., Silcock, G.W.H., and Flood, M. (2002) *Fire Mater* **26**,51-75.

5. Shields, J., Silcock, G.W.H., and Flood, F. (2005) *Fire Technol* **41**,37-65.
6. Skelly, M.J., Roby, R.J., and Beyler, C.L. (1991) *J Fire Prot Eng* **3**,25-34.
7. Keskirahkonen, O. (1988) *Fire Mater* **12**,61-69.
8. Chow, W.K., and Gao, Y. (2008) *Construction and Building Materials* **22**,2157-2164.
9. Xie, Q.Y., Zhang, H.P., Wan, Y.T., Zhang, Q.W., and Cheng, V.D. (2008) *Fire Mater* **32**,293-306.
10. WU, E.M. (1967) *Transactions of the ASME. Journal of Applied Mechanics* **34**,967-974.
11. Wang, Q.S., Zhang, Y., and Sun, J.H. (2012) *under reviewing and first revision returned*.
12. Kamninen, M.F., and Popelar, C.H. (1985). *Advanced fracture mechanics*. Oxford University Press, Oxford.